Journal of Hepatology 2000; **33**: 555–563
Printed in Denmark · All rights reserved
Munksgaard · Copenhagen

Journal of Hepatology
ISSN 0168-8278

Hepatic microvascular features in experimental cirrhosis: a structural and morphometrical study in CCl_4-treated rats

Paolo Onori[1], Sergio Morini[2], Antonio Franchitto[3], Roberta Sferra[1], Domenico Alvaro[4] and Eugenio Gaudio[1]

[1]*Department of Experimental Medicine, Section of Human and Clinical Anatomy, State University of L'Aquila,* [2]*University Campus Bio-Medico, Rome,* [3]*Institute of Human Anatomy, State University of Rome "La Sapienza", and* [4]*Department of Clinical Medicine, Division of Gastroenterology, State University of Rome "La Sapienza", Rome, Italy*

Background/Aims: **In this study, a detailed morphometrical analysis of the hepatic microvasculature in the different zones of hepatic parenchyma was performed in normal and cirrhotic rat liver (CCl_4-induced). The aims were to detect, in CCl_4-induced cirrhosis, the real presence of the "capillarization" of hepatic sinusoids and to assess alterations of the sinusoid/parenchyma ratio within the nodule.**
Methods: **Cirrhosis was promoted by controlled intragastric CCl_4 administration. Scanning electron microscopy of the vascular corrosion cast technique associated with light microscopy and transmission electron microscopy were used.**
Results: **Evidence of connective tissue in the space of Disse was found only in sinusoids located near portal tracts or large fibrotic areas, and this was also confirmed by laminin immunohistochemistry. In contrast, all the intranodular sinusoids lacked real basal membrane and connective fibers in the space of Disse and, displayed normal fenestrations. The parenchymal area, sinusoidal area, mean sinusoidal area, sinusoidal perimeter, hepatocyte area and the reciprocal ratios were all considered in the morphometrical analysis. The sinusoids were of uniform size in the periportal, periseptal and pericentral areas of the cirrhotic liver without the typical zonal differences of the normal liver. The areas occupied by sinusoids per unit of parenchyma and the sinusoid/hepatocyte interfaces disposable for metabolic exchanges were markedly smaller ($p<0.01$) in cirrhotic than normal liver.**
Conclusion: **Our findings indicate that capillarization of hepatic sinusoids occurs only in very limited regions of the cirrhotic parenchyma, and thus this phenomenon does not have relevant functional consequences. Furthermore, the cirrhotic parenchyma appears not to be supplied by sinusoids and lacks features of zonation, which is a condition that could play a major role in the development and progression of liver failure.**

Key words: **Blood vessels; Cirrhosis; Liver; Sinusoids; Ultrastructure.**

LIVER CIRRHOSIS is characterized by the coexistence of necrosis, nodular regeneration and fibrotic septa, which leads to progressive and irreversible hepatic failure. Despite extensive functional and morphological investigations, the mechanisms responsible for the progressive failure of cirrhotic liver are still being debated (1,2). According to the "sick cell hypothesis", progressive hepatocyte cell injury is the main reason for functional liver failure (3,4). Other authors, in contrast, support the functional integrity of hepatocytes (intact cell hypothesis) and the concept that liver failure in cirrhosis is caused by the overall derangement of hepatic structure (5,6). In this second hypothesis, a major role could be played by the pathological changes of the hepatic microvasculature. As early as 1963, Schaffner & Popper (7) described the presence of a capillary basal membrane (CBM) in cirrhotic liver, calling this phenomenon "capillarization" of hepatic sinusoids. Subsequently, other studies (8,9) suggested that modification of the sinusoids could contribute to the impaired exchange of substrates between hepatocytes and blood perfusing the liver. More recently, Martinez-Her-

Received 2 November 1999; revised 10 February; accepted 21 February 2000

Correspondence: Eugenio Gaudio, Department of Experimental Medicine, Section of Human & Clinical Anatomy, Faculty of Medicine, State University of L'Aquila, Via Vetoio, Coppito 2, I-67010 L'Aquila, Italy.
Tel: 39 0862 433504. Fax: 39 0862 433523.
e-mail: gaudio@univaq.it

nandez & Martinez (6) studying plasma clearance and hepatic uptake of different plasma components in normal and cirrhotic rats, reported that CBM in the cirrhotic liver acts as a filtration barrier between plasma and hepatocytes. On the basis of these and other studies, it has been proposed that the "capillarization" of hepatic sinusoids may play a major role in the functional impairment of cirrhotic liver by decreasing the "hepatocyte extraction power".

In addition to the capillarization of hepatic sinusoids, other microvascular abnormalities, such as the altered organization of the cirrhotic nodules for microvessel type (10), shunts between pre- and post-sinusoidal vessels, and the constitution of perinodular plexus (11), have recently been considered to play a role in the impaired hepatic function accompanying the course of cirrhosis. We and others recently focused on the intralobular microvascular rearrangement (11–13) of the cirrhotic liver in relation to metabolic zonation (14–16). In the normal liver, the organization of the microvascular network in the hepatic lobule i.e. vascular pattern (13,17) and regional differences of distribution, types and pattern of sinusoidal fenestration into hepatic lobule (18) plays a key role in determining the histo-functional aspects which are typical of metabolic zonation (16,19). In the cirrhotic nodule, various abnormalities of metabolic zonation have been described, with large differences between the experimental models under investigation. Although it is conceivable that these regional abnormalities are caused by the rearrangement of the microvascular architecture (11,12), detailed studies on the microcirculatory changes in the course of liver cirrhosis, especially those related to intralobular vascular compartmentalization, are scarce.

The aims of this work were to detect, in CCl_4-induced cirrhosis, the real presence of the "capillarization" of hepatic sinusoids in different zones of the cirrhotic nodule and to assess alterations of the sinusoid/parenchyma ratio within the nodule which could justify changes in the metabolic zonation and the loss of the hepatic extractive power which leads to the failure of the hepatic function.

Materials and Methods

Male Wistar rats weighing (ca. 100 g body weight) were divided into control (n=22 rats) and treated (n=32 rats) groups. Samples of rat liver were processed for light microscopy (LM), scanning electron microscopy of vascular corrosion casts (SEMvcc) and transmission electron microscopy (TEM).

Cirrhosis induction

Animals were treated with weekly doses of CCl_4 for 10 weeks according to our previous study (20) and were sacrificed 1 week after the last dose of CCl_4. Barbital sodium was administered to enhance the toxic effects of CCl_4. The National Research Council's criteria for the care and use of laboratory animals were respected in performing this study. Fragments of all the livers (except livers processed for SEMvcc) were taken from the medial lobe, excluding the Glisson's capsule and larger portal branches, and processed for LM and TEM to prove the structural and ultrastructural alterations of micronodular cirrhosis and to perform a morphometrical study.

Light microscopy (LM)

Rat livers were fixed by immersion (10% buffered formalin at room temperature) or by perfusion (n=6 control rats; 8 treated rats) with 2.5% buffered formalin for 30 min (21,22).

Liver samples fixed by immersion were used for routine staining and immunohistochemical studies. The standard procedures for paraffin embedding were used. Five-micrometer-thick sections were stained with hematoxylin-eosin, and Gomori's method for reticular fibers. The samples were observed under a Reichert-Jung Diastar Photomicroscope (Cambridge Instruments, Buffalo, New York, USA).

Livers fixed by perfusion were used for morphometrical studies (see above).

Immunohistochemistry (IHC)

Liver samples, were fixed by immersion as described above for LM and embedded in 55–57°C melting point paraffin. Sections (3–4-mm-thick) were mounted on glass slides coated with 0.1% poly-L-lysine (Sigma P-1524). After deparaffination in xylene, absolute alcohol and 95% alcohol, endogenous peroxidase activity was blocked by a 30-min incubation in 2.5% methanolic hydrogen peroxide. Sections were hydrated in graded alcohol and phosphate-buffered saline (PBS, pH 7.4) before applying the primary antibody. After predigestion with pepsin 1 mg/ml 0.01N HCl at 37°C for 5 min, sections were incubated overnight at 4°C with laminin polyclon antibody (BioGenex lab cat #PU078-UP) diluted 1:20. Samples were then rinsed with TRIS for 5 min and incubated for 10 min at room temperature with secondary biotinylated antibody (Dako LSAB 2 kit; cod. K0675). After rinsing in TRIS for 15 min, the sections were incubated for 10 min with Dako ABC, washed again in TRIS and finally developed with 3-3' diaminobenzidine (DAB). Negative and positive controls were included in each bath of slides. The samples were counterstained with hematoxylin. All IHC reactions were observed using a Reichert-Jung Diastar photomicroscope (Cambridge Instruments, Buffalo, NY, USA).

Transmission electron microscopy (TEM)

Fragments of the central zone of the medial lobe of the liver were taken from control and treated rats. The samples were fixed in 2.5% glutaraldehyde in 0.1 M Sorensen's phosphate buffer solution pH 7.4, at 4°C for 24 h and postfixed in 2% buffered OsO_4 for 2 h. After dehydration in alcohol, the samples were embedded in Agar 100 (Agar Scientific, Stansted, UK) for 48 h at 60°C. Semi-thin sections (1–1.5 μm) were obtained with a glass knife on a Top Ultra 170 ultramicrotome (Pabisch, Milan, Italy), stained with methylene blue and observed under light microscope for selecting representative areas.

In the cirrhotic livers the following three areas were selected: a) the area localized near the portal tract (Rappaport's zone 1 in normal liver), called the "periportal" area; b) the area localized near the newly formed portocentral connective septa at equal distance from the portal space and central vein (Rappaport's zone 2 in normal liver), called the "periseptal" (intermediate) area; and, c) the area near the centrolobular vein (Rappaport's zone 3 in normal liver), called the "pericentral" area.

In normal livers three areas were selected according to Rappaport's zone 1, 2 and 3.

Thin sections obtained with a diamond knife were stained with uranyl acetate and lead citrate and then examined with a Zeiss EM 9A transmission electron microscope (Carl Zeiss, Oberkochen, Germany).

Scanning electron microscopy vascular corrosion casts (SEMvcc)

After an ether/air blend of anesthesia, the abdomen of the rat was opened and a cannula (Inpharven® diameter 1.4 mm) was inserted

into the aorta and fixed with 2 silk ties. Before flushing the vascular bed with heparinized 0.9% saline solution (23,24), the thorax was opened and the right atrium incised to allow the efflux of the perfusate. When the outflow fluid appeared clear of blood, Mercox CL2R resin diluted with methyl methacrylate monomer (4:1) (25), mixed with a standard amount of its catalyser (up to 2 ml catalyser) per 20 ml of base compound) was injected at room temperature. A constant pressure control was maintained (CONEL electronic manometer, Rome, Italy) through the lateral port of the cannula's injection valve until resin polymerization was visible (26). The animals were left at room temperature for 24 h and after the polymerization of the resin, the livers were removed and macerated in 20% NaOH solution at room temperature. After rinsing in distilled water, the liver casts were placed in 5% trichloroacetic acid (CCl_3COOH) solution to free the cast from tissue remnants. The casts were isolated, frozen in distilled water and freeze-dried. They were then glued onto stubs by means of Silver Dag and gold coated in an S150 sputterer (Edwards, London, UK). Finally, the prepared casts were examined with a Hitachi S4000 field emission scanning electron microscope (Hitachi Ltd., Tokyo, Japan) operating at 5–8 kV.

Morphometry

For morphometrical studies, 6 normal and 8 cirrhotic rats were fixed by perfusion (22) with 2.5% buffered formalin for 30 min, in order to obtain rapid fixation of sinusoid walls. Thereafter, the liver was removed and fixed by immersion in 2.5% buffered formalin for 60 min. Morphometric study of the livers was performed using liver fragments taken from the medial lobe, excluding Glisson's capsule and larger portal branches. Six rats from the control group and eight from the CCl_4-treated group were sacrificed. Six different blocks were randomly prepared (from each rat of both control and treated groups) and the measurements were obtained with a Kontron MOP Videoplan image analyzer (Kontron, Milan, Italy) on light micrographs by paraffin sections, according to Loud (27) and Weibel et al. (28).

Morphometrical analysis of the hepatic structure was carried out on the following zones:

a. *Control livers:* Periportal (Rappaport's zone 1), Intermediate (Rappaport's zone 2) and pericentral (Rappaport's zone 3);
b. *Treated livers:* Periportal (area near portal tract); periseptal (area localized near the neo-formed portocentral connective septa equidistant from portal tract and former central vein) and pericentral (area near the former central vein).

The following data were assessed for each zone:

1. *Parenchymal area (PA):* Sum of all the surfaces observed;
2. *Sinusoidal area (SA):* Sum of all the sinusoidal surfaces observed;
3. *Mean sinusoidal area (MSA):* Sinusoidal area (of each field studied)/total number of sinusoids;
4. *Hepatocyte area (HA):* Sum of all the hepatocyte surfaces observed;
5. *Sinusoidal perimeter (SP):* Sum of length of the sinusoidal border;
6. *SA/PA ratio:* Ratio between the sinusoidal area and the parenchymal area. The ratio indicates the parenchymal space occupied by the sinusoids (high value ratio=more sinusoids present, low value ratio=more hepatocytes present);
7. *SA/SP index:* Obtained by dividing the sinusoidal area by the sinusoidal perimeter (high value index=tendency to larger shape of sinusoids; low value index=tendency to a narrow and lengthened shape of the sinusoids);
8. *HA/SP index:* Obtained by dividing the hepatocyte area by the sinusoidal perimeter. This index shows the hepatocyte surface joined to the unity of length of sinusoids (high value index=lower interface between hepatocytes and sinusoids, useful for exchanges).

All morphological and morphometrical evaluations were done double-blind.

Statistical analysis

Statistical analysis was performed using Student's *t*-test or the analysis of variance (Anova) when multiple comparisons were performed.

Results

LM

Control rats showed a normal structure of the liver (Fig. 1a). Features of micronodular cirrhosis were always present in CCl_4-treated livers (Fig. 1b). The major alterations of the liver structure consisted of: i) increased connective tissue in the portal spaces; ii) the presence of fibrous septa originating from portal spaces, which often connected portal spaces among them and with the central vein; iii) small septa extending from the central vein into the neighboring parenchyma. Bi-, or tri-stratified laminae of hepatocytes were sometimes present in micronodular parenchyma.

Silver impregnation with Gomori's method allowed the visualization of argyrophylia of the reticular and connective tissue fibers. This was evident in both normal and cirrhotic livers near large vessels and, in cirrhotic livers, close to the large connective tissue septa. In addition, it appeared wavy and discontinuous inside

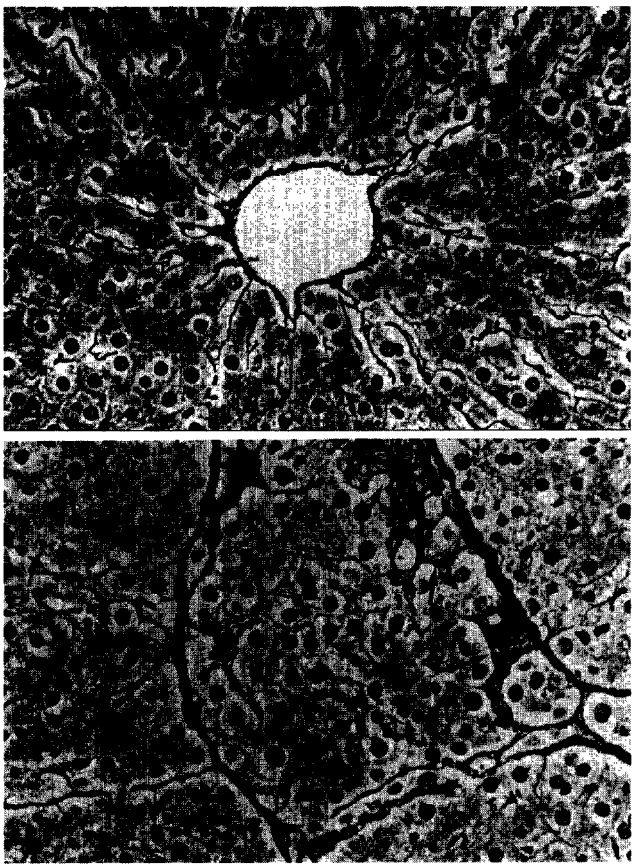

Fig. 1. L.M., 200×, Gomori reticulum stain. a. Normal rat liver. A normal hepatic structure is evident. b. Cirrhotic rat liver. After 10 weeks of CCl_4, the connective septa crosses the liver parenchyma forming micronodules. Inside the nodules the argyrophylia appears discontinuous and more evident near large septa (arrows).

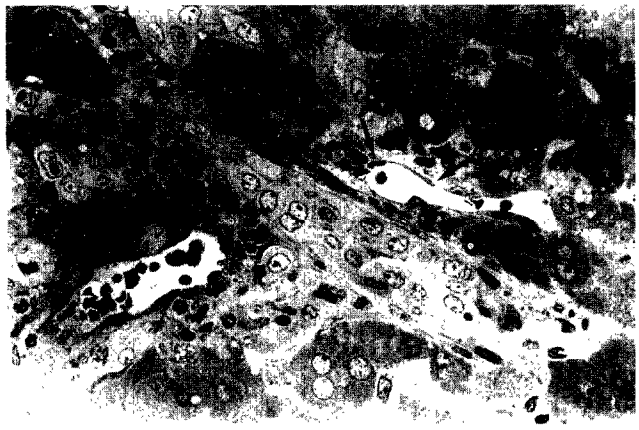

Fig. 2. L.M., 200×, semi-thin section, methylene blue stain. Cirrhotic rat liver. The presence of vessels close to the septa which are encircled by connective tissue (arrows) is evident.

the hepatic lobule or the cirrhotic nodule. In the cirrhotic liver, only limited small vessels, close to the portal space and septa, appeared encircled by a thin connective tissue (Fig. 2).

IHC

The immunoreaction for laminin in normal liver was detected only at the level of portal tracts and around the major central veins (Fig. 3a).

In cirrhotic liver, a clear positivity for laminin was detected at the level of portal tract or large connective septa (Fig. 3b). Inside the nodule, the space between the sinusoids and hepatic trabeculae showed no reaction (Fig. 3b).

TEM

TEM observations were focused on the perisinusoidal spaces of the hepatic parenchyma in all the selected zones of control and CCl_4-treated livers.

Normal architecture of the sinusoidal wall was observed in control livers.

Cirrhotic livers, in turn, showed more connective tissue in the space of Disse only in the sinusoids located close to the portal spaces or to the large connective septa. Therefore, the phenomenon of capillarization was limited to these areas.

In the three nodular zones examined (i.e. periportal, pericentral and periseptal) the endothelium formed a very thin barrier between the sinusoidal lumen and the perivascular space (Fig. 4a). In all the samples studied, it was possible to observe small fenestrations in the endothelium connecting the sinusoidal lumen to the space of Disse (Fig. 4b). The vascular surface of the hepatocytes presented numerous irregularly oriented microvilli projecting into the perivascular space (Fig. 4a).

SEM vcc

SEMvcc permitted a detailed 3D observation of the vascular network, and a simple differentiation of arterial and venous vessels.

In the normal liver, the sinusoids formed a continuous network of regular diameter (Fig. 5a). A large portal vein, a small hepatic artery and sometimes a peribiliary plexus were observed in the portal tract. On the opposite side, the sinusoids mostly ran into the central vein at right angles.

In CCl_4-treated livers the microvascular features corresponded to well-structured nodules of spherical shape (Fig. 5b). Among the nodules, a space containing large sublobular vessels was present and formed a perinodular plexus (Fig. 5b). These vessels showed characteristics of both afferent and efferent vessels.

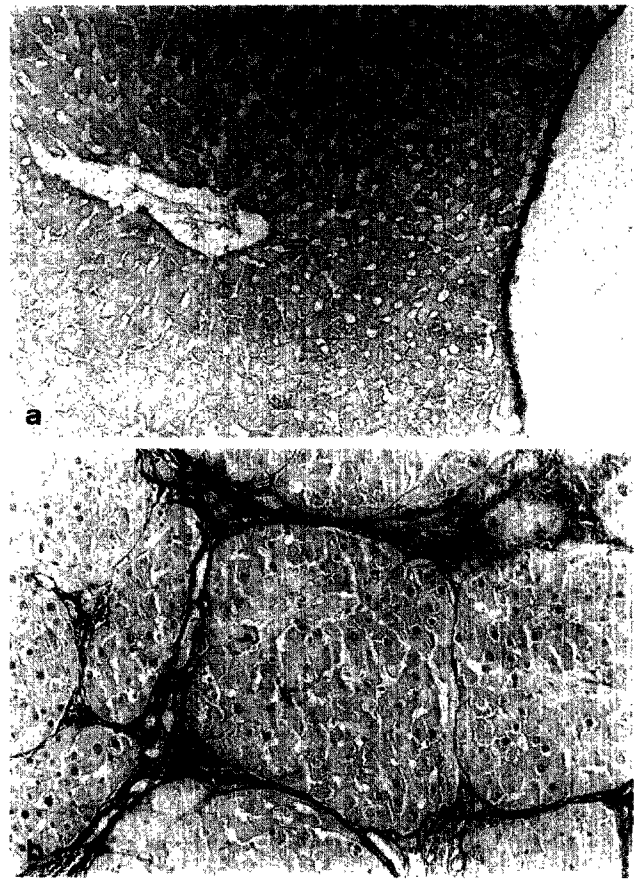

Fig. 3. I.H.C., 160×, laminin immunoreaction. a. Normal rat liver. Evident immunostaining is observed around the large central vein. b. Cirrhotic rat liver. Strong positivity is evident along the connective tissue septa that crosses the liver parenchyma forming micronodules. Inside the nodules the parenchyma appeared negative.

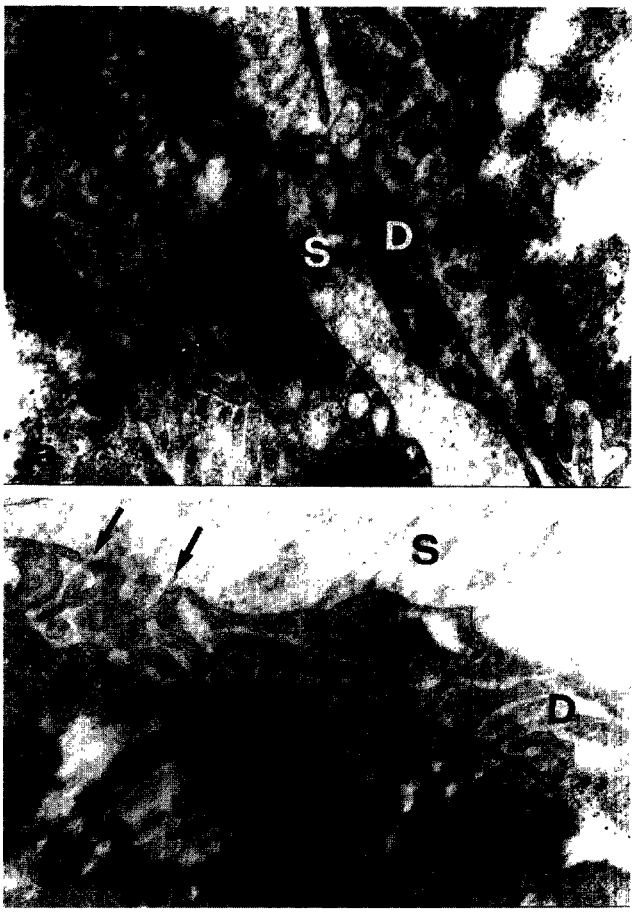

Fig. 4. T.E.M. (a=16 000×; b=20 000×). Cirrhotic rat liver. The hepatic ultrastructure showed the absence of fibrosis around a sinusoid (S). The sinusoid's endothelium appears interrupted (arrow). At high magnification (b), small fenestrations in the endothelium (arrow heads) which connect the sinusoidal lumen with the space of Disse (D) are evident. m=mitochondrion.

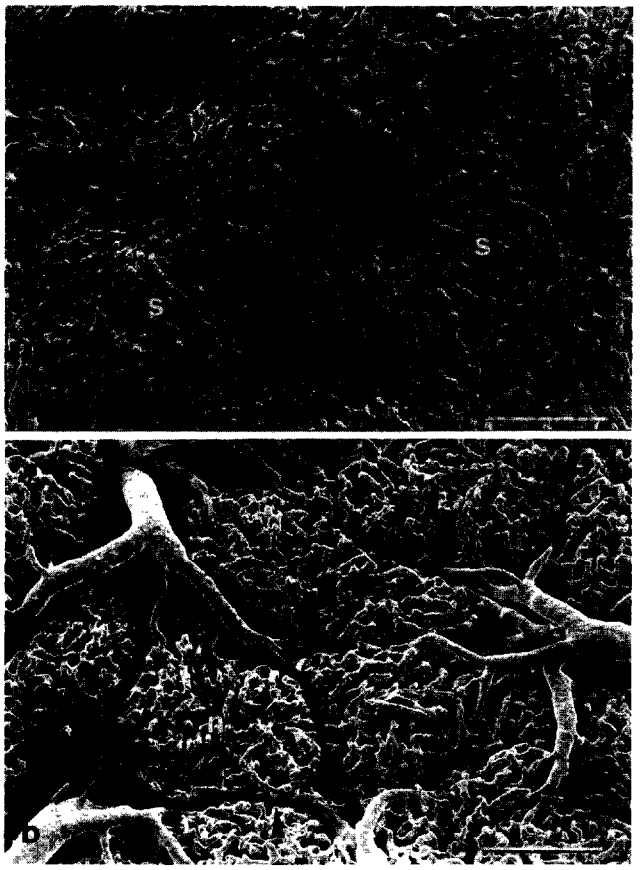

Fig. 5. S.E.M.v.c.c. a. Control rat liver (bar=100 μm). Normal vascularization of the surface hepatic parenchyma with a continuous network of sinusoids (s) is evident. b. Cirrhotic rat liver (bar=100 μm). Micronodules (n) separated by empty space (arrow head) (corresponding to macerated septa) are evident. Some large vessels run around the nodule forming a perinodular plexus (arrow).

They sometimes appeared flattened and dead-ended, indicating vascular proliferation. The presence of the central vein inside the sinusoidal nodule could not be observed, so the radial appearance of sinusoids around the vessel observed in normal livers was completely lost.

Morphometry

The morphometrical data from normal and cirrhotic livers are reported in detail in Tables 1 and 2.

In the normal liver, the sinusoidal area/parenchymal area (SA/PA) ratio appeared different in the three studied zones. While similar values were observed in the periportal and intermediate zones (11.97% and 11.49%), the SA/PA ratio appeared 70% greater ($p<0.01$) in the pericentral zone (20.14%; Table 1). Moreover, the sinusoids in the pericentral area were larger, with a 2-fold higher mean sinusoidal area ($p<0.01$) and a higher ($p<0.01$) sinusoidal area-perimeter (SA/SP) index, indicating the tendency of sinusoids to assume a larger aspect in the pericentral zone compared to the periportal or intermediate zone.

In contrast, the hepatocyte area-sinusoidal perimeter (HA/SP) index, which indicates the hepatocyte surface (as it appears in a micrograph) served by the sinusoidal perimeter, showed a higher value ($p<0.01$) in the periportal and intermediate zones (14.88 and 15.22, respectively) compared to the pericentral area (9.26). The high value of this parameter indicated the presence of a lower interface disposal for metabolic exchanges between hepatocytes and sinusoids. As a consequence, in normal livers the hepatocytes-sinusoids interface was larger in the pericentral than in the other zones.

TABLE 1

Morphometrical data on histological sections from normal livers

	Periportal area (Rappaport's zone 1)	Intermediate area (Rappaport's zone 2)	Pericentral area (Rappaport's zone 3)
Observations (number)	36	36	36
Parenchymal area (PA)	421 197±11 286 μ^2	436 644±3 709 μ^2	422 320±15 668 μ^2
Sinusoidal area (SA)	50 767±2 874 μ^2	50 320±3 538 μ^2	85 155±6 184 μ^{2*}
Mean sinusoidal area	231.63±28.94 μ^2	212.99±23.65 μ^2	413.01±81.32 μ^{2*}
Hepatocyte area (HA)	370 431±12 335 μ^2	390 662±3 649 μ^2	337 165±14 532 μ^{2*}
Sinusoidal perimeter (SP)	24 909±2 069 μ	25 675±1 294 μ	36 410±3 073 μ^*
SA/PA ratio×100	11.97±0.62	11.49±1.12	20.14±1.49*
SA/SP index	2.02±0.12	1.95±0.15	2.33±0.28*
HA/SP index	14.88±1.13	15.22±0.84	9.26±0.81*

Data are mean±SD from n=6 rats. *=$p<0.01$ *vs* periportal or intermediate area.

TABLE 2

Morphometrical data on histological sections from cirrhotic livers

	Periportal area	Periseptal area	Pericentral area
Observations (number)	48	48	48
Parenchymal area (PA)	315 575±25 863 $\mu^{2\,\&}$	369 197±14 638 $\mu^{2\,\&}$	323 740±10 786 $\mu^{2\,\&}$
Sinusoidal area (SA)	30 225±4 584 $\mu^{2\,\&}$	33 646±3 463 $\mu^{2\,\&}$	37 992±2 815 $\mu^{2\,\&*}$
Mean sinusoidal area	235.60±58.32 μ^2	237.12±64.57 μ^2	288.09±75.15 $\mu^{2\,\&}$
Hepatocyte area (HA)	285 351±26 037 $\mu^{2\,\&}$	335 552±14 853 $\mu^{2\,\&}$	285 748±10 247 $\mu^{2\,\&}$
Sinusoidal perimeter (SP)	14 515±2 063 $\mu^{\&}$	15 482±1 326 $\mu^{\&}$	18 820±1 214 $\mu^{\&*}$
SA/PA ratio×100	9.54±1.33	9.10±1.5$^{\&}$	11.72±0.84$^{*\&}$
SA/SP index	2.07±0.12	2.17±0.23	2.01±0.10$^{\&}$
HA/SP index	19.66±2.24$^{\&}$	21.67±2.51$^{\&}$	15.18±1.07$^{*\&}$

Data are mean±SD from n=8 rats. *$p<0.01$ *vs* periportal or periseptal area. $^{\&}$=$p<0.01$ *vs* corresponding values of the control normal liver (see Table 1 for comparison).
Parenchymal area (PA): sum of all the surfaces observed; Sinusoidal area (SA): sum of all the sinusoidal surfaces observed; Mean sinusoidal area (MSA): sinusoidal area (of each field studied)/total number of the sinusoids; Hepatocyte area (HA): sum of all the hepatocyte surfaces observed; Sinusoidal perimeter (SP): sum of length of the sinusoidal border; Sinusoidal area/Parenchymal area (SA/PA): ratio between the sinusoidal area and the parenchymal area. The ratio is an index of the parenchymal space occupied by the sinusoids (high value ratio=more presence of sinusoids, low value ratio=more presence of hepatocytes); Sinusoidal area/sinusoidal perimeter index (SA/SP): ratio between the sinusoidal area and the sinusoidal perimeter. This ratio is an index of the sinusoidal surface joint to the unity of length of sinusoids (high value ratio=tendency to larger shape of sinusoids, low value ratio=tendency to a narrow and lengthened shape of sinusoids); Hepatocyte area/sinusoidal perimeter index (HA/SP): ratio between the hepatocyte area and the sinusoidal perimeter. This ratio is an index of the hepatocyte surface joint to the unity of length of sinusoids (high value ratio=lower interface between hepatocytes and sinusoids useful for exchanges).

In the cirrhotic liver, the sinusoidal area and the ratio between the sinusoidal and the parenchymal area (SA/PA) tended to be homogeneous in all the three studied zones. In fact, the SA/PA ratio in the pericentral zone was only 22–28% higher (11.72%) than in the other zones, (9.54% (periportal) and 9.10% (periseptal). The sinusoidal area and the SA/PA ratio were significantly ($p<0.01$) lower in cirrhotic compared to normal livers. This difference was much more evident in the pericentral zone. These data indicated the presence of fewer sinusoids in the cirrhotic parenchyma and a smaller space occupied by blood per unit of parenchyma.

In the cirrhotic liver, the mean sinusoidal area and the sinusoidal area/sinusoidal perimeter index showed similar values in the three zones studied. Thus, the zonal differences of the normal liver (higher mean sinusoid area and SA/SP index in pericentral area) were lost in cirrhosis. This indicated that sinusoids were homogeneously distributed in the cirrhotic liver without the morphological zonation of the normal liver.

The HA/SP index was markedly higher ($p<0.01$) in the cirrhotic liver, compared to the normal liver and this phenomenon was equally evident in all three zones. This indicated that the interface available for metabolic exchange was seriously decreased during liver cirrhosis.

Discussion

The main findings emerging from this study on CCl_4-induced cirrhosis are that: 1) features of capillarization (real basal membrane and connective tissue in the space of Disse) are only evident in the sinusoids located near the portal spaces or close to the large con-

nective septa. In contrast, features of capillarization are lacking in all intranodular sinusoids, as demonstrated by the absence of a real basal membrane, the space of Disse free of connective fibers and the presence of fenestrations in the sinusoidal endothelium; 2) sinusoids tend to show uniform morphometric features in periportal, periseptal and pericentral zones without the marked zonal differences of the normal liver; 3) the areas occupied by sinusoids per unit of parenchyma and the interfaces sinusoids/hepatocytes available for metabolic exchanges are markedly smaller than in the normal liver.

The CCl_4-treated rat is a well-standardized and reproducible experimental model (20,29) which has been widely used for functional and morphologic studies on the cirrhotic liver in the last few years. Within the different experimental models, the CCl_4 is, from a morphological point of view, the most similar to human cirrhosis (20,29,30). This model allows the performance of detailed structural and ultrastructural observations on selected and homogeneous areas of parenchyma, taken from the same lobe of each liver at an equal distance from the capsule and larger portal branches (11,13,16).

The transformation of hepatic sinusoids into capillaries during cirrhosis, originally called "capillarization" (7), represents a morphological alteration supposed to explain impaired exchanges of substrates between plasma and hepatocytes. Although a continuous endothelium and basal membranes (BMs) in cirrhotic livers have been observed by different authors (6,31–33), these observations have not been systematically correlated with recent knowledge on the microvascular and metabolic zonation of the cirrhotic nodule (14,15,19). While studying the capillarization of sinusoids, in both normal and cirrhotic samples, it is important to consider which zone is observed and the distance between the main connective septa and Glisson's capsule. Moreover, as already observed by Rappaport (34), it is important to take into consideration that nodules appear heterogeneous and that many microvessels remain typical sinusoids within the nodules. In our TEM observations, we failed to observe the presence of a real and continuous basal membrane in the major part of the sinusoidal wall in the three selected zones of the cirrhotic nodule. Moreover, the spaces of Disse were free from connective tissue fibers, and fenestrations were present in the sinusoidal endothelium. The immunohistochemical localization of laminin, a major component of basal membrane (35), further confirmed that the basement membrane, a hallmark of capillarization (35), was confined to the level of large portal tracts or in the vessels running in large connective septa of cirrhotic livers, while it was absent inside the nodules.

Therefore, real capillarization is lacking in a large part of the nodules despite a clear and morphologically documented cirrhotic transformation of the liver. Vessels encircled by a thin connective tissue were observed only in the area located near the portal zones and large connective septa, which indicates that capillarization is confined to a very limited part of the cirrhotic parenchyma. As a consequence, capillarization cannot be considered a major reason for the altered hepatic uptake of plasma components and for the progressive and irreversible hepatic failure.

Instead, other microvascular pathological changes of the cirrhotic liver may play a major role in the decreased extraction power and the progressive liver failure. In fact, our morphometrical data show that in periportal, periseptal and pericentral zones, the sinusoids tend to display homogeneous morphometric features without the wide differences in mean sinusoidal area and SA/SP index which are typical of the selected zones of the normal liver. Therefore, the pressure gradient which characterizes blood flow inside the normal lobule (31–34) could be reduced in the cirrhotic nodule due to the loss of the angioarchitectural zonation. Moreover, perinodular shunts between the portal and the centrolobular veins can develop and grow into the connective septa which surround the nodule. These data are correlated with the vascular corrosion casts observed by SEM. The 3-D organization of the nodules is composed of a core of sinusoids (11,12,36) without evident morphological alterations in the sinusoidal lining, and is surrounded by larger vessels which form the perinodular plexus. In particular, the new developing vessels, which contribute to the formation of the perinodular plexus, often connect afferent and efferent vessels (11). The decreased sinusoidal area is one major factor involved in the development of portal hypertension, together with impaired sinusoidal wall elasticity and abnormal regulation of vascular resistance by endothelin and nitric oxide (37–39).

The main finding of the morphometrical study is that the HA/SP index, which represents the hepatocyte-plasma interchange surface, was constantly higher in cirrhotic livers. As a consequence, the perfusion ratio was seriously impaired in cirrhotic livers because of reduced vascularization in relation to the hepatocyte mass. The decreased parenchymal perfusion, which is due to the loss of the regular and continuous network of the converging sinusoids to the central vein, and the presence of two or three stratified laminae of hepatocytes, could explain the associated alteration in the normal metabolic zonation. In fact, the typical zonal

distribution of the most important hepatic enzymes present in normal liver (16,19,36) is attenuated in the cirrhotic liver, together with loss of ultrastructural differences between hepatocytes from the periportal, periseptal and pericentral areas (16).

In normal liver, the functional difference between cells (metabolic zonation) is determined or influenced by the spatial orientation of the blood supply and/or by regional differences in the path of the diffusion of oxygen, substrates and hormones (40,41). The partial oxygen pressure in the rat liver has been reported to grade from the periportal to the perivenous zone and this may influence the regional differences in the oxidative energy metabolism, as well as in the regeneration after liver injury ("streaming liver") (42). In the cirrhotic liver, the dramatic changes in parenchymal perfusion may well justify the pathological changes in the functional and ultrastructural zonation (16) and may influence the progression of liver failure. In fact, the intranodular sinusoidal bed, which lacks a zonal compartmentalization, may become progressively insufficient to adequately supply the functional demands of the hepatocyte mass. The overall reduction of sinusoidal area compared with parenchymal mass could suggest a failure of neovascularization in the cirrhotic liver. Although a recent study indicates that the serum levels of vascular endothelial growth factor (VEGF) are decreased in patients with liver cirrhosis compared with in normal controls (43), the relevance of these data in the absence of information concerning VEGF hepatic levels or receptor status in liver cells is doubtful. However, in cirrhotic liver new vessels develop all around the nodule and follow neoformed septa, as demonstrated by SEMvcc (11,12,16), while inside the nodule the hepatocyte proliferation does not respect the tidy sequence of sinusoids and cell laminae which characterize the normal lobule. Concerning the above points, we believe that the discrepancy between the parenchymal mass and the sinusoidal bed is due mainly to the abnormal hepatocyte proliferation rather than a failure of neovascularization in cirrhotic livers.

The architectural microvascular changes described in the CCl_4 model are completely different from those in cirrhosis secondary to bile duct obstruction where hepatic sinusoids showed a regular organization and there were no significant pattern modifications in comparison to normal liver (44). In particular, the microvasculature changes in cirrhosis secondary to bile duct obstruction appeared to be restricted to the peribiliary plexus. This could explain the delayed occurrence of liver failure in primary biliary cirrhosis compared to common cirrhosis. Unfortunately, microvascular studies in other experimental models of cirrhosis are not available.

Our findings may have a number of physiopathological implications. First, the decreased parenchymal perfusion and the intrahepatic vascular shunts, by decreasing the extraction power, may favor the hyperammonemia and impaired protein synthesis which characterize the progression of the disease. Second, the hepatocyte mass works in a condition of low perfusion, thus favoring the generation and accumulation of peroxidation products, which in turn determine or accelerate the progression of fibrosis (45). Third, a significant part of the hepatic parenchyma, especially the part which is distant from the vascular bed, receives a very low amount of hormones and may thus escape the hormonal regulation of metabolic functions.

In conclusion, capillarization of the sinusoids is absent within the nodule. The rearrangement of the hepatic structure in CCl_4 cirrhosis in the rat leads to a loss of the metabolic zonation and is associated with relevant morphological and quantitative alterations of the microvascolature, with a marked decrease of sinusoid/hepatocyte interfaces disposable for metabolic exchanges. Thus, the reduced vascularization in relation to parenchymal mass progressively becomes insufficient to successfully supply the functional needs of the hepatocytes, and may play a major role in the development of liver failure.

Acknowledgements

This study was supported by funds from Italian M.U.R.S.T. (40% and 60%) and C.N.R.

References

1. MacSween RNM, Anthony PP, Scheuer PJ. Pathology of the Liver. Edinburgh: Churchill Livingstone; 1987. p. 342–63.
2. Schiff L, Schiff ER. Diseases of the Liver. Philadelphia: JB Lippincott; 1993.
3. Pessayre D, Lebrec D, Descatoire V, Peignoux M, Benhamou JP. Mechanism for reduced drug clearance in patients with cirrhosis. Gastroenterology 1978; 74: 566–71.
4. Reichen J, Hoilien C, Le M, Jones RH. Decreased uptake of taurocholate and ouabain by hepatocytes isolated from cirrhotic rat liver. Hepatology 1987; 7: 67–70.
5. Vaubourdolle M, Guffet V, Guecho J, Ballet F, Jaillon P, Giboudeau J, et al. Evidence of the intact hepatocyte theory in alcoholic cirrhosis. Scand J Gastroenterol 1989; 24: 467–74.
6. Martinez-Hernandez A, Martinez J. The role of capillarization in hepatic failure: studies in carbon tetrachloride-induced cirrhosis. Hepatology 1991; 14: 864–74.
7. Schaffner F, Popper H. Capillarization of hepatic sinusoids in man. Gastroenterology 1963; 44: 239–42.
8. Martinez-Hernandez A. The hepatic extracellular matrix. I. Electron immunohistochemical studies in normal rat liver. Lab Invest 1984; 51: 57–74.
9. Martinez-Hernandez A. The hepatic extracellular matrix. II. Electron immunohistochemical studies in rats with CCl_4-induced cirrhosis. Lab Invest 1985; 53: 166–86.
10. Rappaport AM, Macphee PJ, Fischer MM, Phillips MJ. The scarring of the liver acini (cirrhosis): tridimensional and microcirculatory considerations. Virchows Arch (A) 1983; 402: 107–37.

11. Gaudio E, Pannarale L, Onori P, Riggio O. A scanning electron microscopic study of liver microcirculation disarrangement in experimental rat cirrhosis. Hepatology 1993; 17: 477–85.
12. Haratake J, Hisaoka M, Yamamoto O, Horie A. Morphological changes of hepatic microcirculation in experimental rat cirrhosis: a scanning electron microscopic study. Hepatology 1991; 13: 952–6.
13. Gaudio E, Pannarale L, Ripani M, Onori P, Riggio O. The hepatic microcirculation in experimental cirrhosis. A scanning electron microscopy study of microcorrosion casts. Scan Microsc 1991; 5: 495–503.
14. Sokal EM, Trivedi P, Portman B, Mowat AP. Adaptative changes of metabolic zonation during the development of cirrhosis in growing rats. Gastroenterology 1990; 99: 785–92.
15. Sokal EM, Mostin J, Buts JP. Liver metabolic zonation in rat biliary cirrhosis: distribution is reverse of that in toxic cirrhosis. Hepatology 1992; 5: 904–8.
16. Gaudio E, Onori P, Franchitto A, Sferra R, Riggio O. Liver metabolic zonation and hepatic microcirculation in carbon tetrachloride-induced experimental cirrhosis. Dig Dis Sci 1997; 42: 167–77.
17. Ohtani O. The microvascularization of the liver, the bile duct and the gallbladder. In: Motta PM, editor. Biopathology of the Liver: an Ultrastructural Approach. Dordrecht, The Netherlands: Kluwer Academic Publisher; 1988. p. 83–97.
18. Shin YC. Revaluation on the types and pattern of distribution of sinusoidal fenestrations in the lobule of normal rat liver. Anat Rec 1997; 247: 206–13.
19. Sokal EM, Trivedi P, Cheeseman P, Portman B, Mowat AP. The application of quantitative cytochemistry to study the acinar distribution of enzymatic activities in human liver biopsy sections. J Hepatol 1989; 9: 42–8.
20. Ariosto F, Riggio O, Cantafora A, Colucci S, Gaudio E, Mechelli C, Merli M, et al. Carbon tetrachloride-induced experimental cirrhosis in the rat: a reappraisal of the model. Eur Surg Res 1989; 21: 280–6.
21. Motta P, Porter KR. Structure of rat liver sinusoid and associated tissue spaces as revealed by scanning electron microscopy. Cell Tissue Res 1974; 148: 11–125.
22. Carpino F, Gaudio E, Marinozzi G, Melis M, Motta PM. A scanning and transmission electron microscopic study of experimental extrahepatic cholestasis in the rat. J Submicrosc Cytol 1981; 13: 581–8.
23. Hodde KC, Miodonski A, Bakker C, Veltman WAM. SEM of microcorrosion casts with special attention on arterio-venous differences and application to the rat cochlea. Scanning Electron Microscopy 1977; II: 477–84.
24. Miodonski AJ, Jasinski A. SEM study of microcorrosion casts of the vascular bed in the skin of the spotted salamander. Cell Tiss Res 1979; 196: 153–62.
25. Lametschwandtner A, Lametschwandtner U, Weiger T. Scanning electron microscopy of vascular corrosion casts. Technique and applications: updated review. Scanning Mic 1990; 4: 889–941.
26. Pannarale L, Onori P, Ripani M, Gaudio E. Retinal microcirculation as revealed by SEM corrosion casts in the rat. Eur J Ophthalmol 1991; 1: 96–102.
27. Loud AV. A quantitative stereological description of the ultrastructure of normal rat liver parenchymal cells. J Cell Biol 1968; 37: 27–46.
28. Weibel ER, Staubli W, Gnagi IR, Hess FA. Correlated morphometric and biochemical studies on the liver cell. J Cell Biol 1969; 12: 68–91.
29. Proctor E, Chatamra K. Standardized micronodular cirrhosis in the rat. Eur Surg Res 1984; 16: 182–6.
30. Cameron GR, Karunaratne WAE. Carbon tetrachloride cirrhosis in relation to liver regeneration. J Path Bact 1936; 42: 1–21.
31. Huet PM, Goresky CA, Villeneuve JP, Marleau D. Assessment of liver microcirculation in human cirrhosis. J Clin Invest 1982; 70: 1234–44
32. Huet PM, Pomier-Layrargues G, Villeneuve JP, Varin F, Viallet A. Intrahepatic circulation in liver disease. Semin Liver Dis 1986; 6: 277–86.
33. Varin F, Huet PM. Hepatic microcirculation in the perfused cirrhotic rat liver. J Clin Invest 1985; 76: 1904–12.
34. Rappaport AM. Hepatic blood flow. In: Javit NB, editor. Liver and Biliary Tract Physiology I. Intern Rev Physiol, vol. 21. Baltimore: University Park Press; 1980. p. 1–63.
35. Martinez-Hernandez A, Amenta PS. The extracellular matrix in hepatic regeneration. FASEB J 1995; 9: 1401–10.
36. Haratake J, Yamamoto O, Hisaoka M, Horie A. Scanning electron microscopic examinations of microvascular casts of the rat liver and bile duct. JUOEH 1990; 12: 19–28.
37. Shibayama Y. On the pathogenesis of portal hypertension in cirrhosis of the liver. Liver 1988; 8: 95–9.
38. Leivas A, Jimenez W, Bruix J, Boix L, Bosch L, Arroyo V, et al. Gene expression in endothelin-1 and ET(A) and ET(B) receptors in human cirrhosis: relationship with hepatic hemodynamics. J Vasc Res 1998; 35: 186–93.
39. Rochey DC, Chung JJ. Reduced nitric oxide production by endothelial cells in cirrhotic rat liver: endothelial dysfunction in portal hypertension. Gastroenterology 1998; 114: 344–51.
40. Kats N, Jungermann K. Metabolic heterogeneity of the liver. In: Tavoloni N, Berk PD, editors. Hepatic Transport and Bile Secretion: Physiology and Pathophysiology. New York: Raven Press; 1993. p. 55–70.
41. Seifter S, Englard S. Energy metabolism. In: Arias IM, Bioyer JL, Fausto N, Jakoby WB, Schachter D, Shafritz DA, editors. The Liver. Biology and Pathobiology, 3rd ed. New York: Raven Press; 1994. p. 323–64.
42. Seifter S, Fausto N. Liver stem cells. In: Arias IM, Bioyer JL, Fausto N, Jakoby WB, Schachter D, Shafritz DA, editors. The Liver. Biology and Pathobiology, 3rd ed. New York: Raven Press; 1994. p. 1501–18.
43. Akiyoshi F, Sata M, Suzuki H, Uchimura Y, Mitsuyama K, Matsuo K, et al. Serum vascular endothelial growth factor levels in various liver diseases. Dig Dis Sci 1998; 43: 41–5.
44. Gaudio E, Onori P, Pannarale L, Alvaro D. Hepatic microcirculation and peribiliary plexus in experimental biliary cirrhosis: a structural and ultrastructural study in the rat. Gastroenterology 1996; 111: 1118–24.
45. Greenwel P, Geerts A, Ogata I, Solis-Herruzzo J-A, Rojkind M. Liver fibrosis. In: Arias IM, Bioyer JL, Fausto N, Jakoby WB, Schachter D, Shafritz DA, editors. The Liver. Biology and Pathobiology, 3rd ed. New York: Raven Press; 1994. p. 367–82.